Research Article

Ex Vivo Modelling of Therapy Efficacy for Rare Krukenberg Tumors – A Report of Two Cases

Antti Arjonen[1,2#], Rami Mäkelä[1], Reetta Virtakoivu[3,4#], Ville Härmä[1,7#], Teijo Kuopio[5], Heikki Hakkarainen[5], Maija Hollmén[3], Juha Kononen[5,6#] and Juha K. Rantala[1,7]*

[1]*Misvik Biology Ltd, Turku, Finland*

[2]*Brinter Ltd, Turku, Finland*

[3]*MediCity Research Laboratory, Institute of Biomedicine, Faculty of Medicine, University of Turku, Turku, Finland*

[4]*Orion Corporation Orion Pharma, Espoo, Finland*

[5]*Central Finland Health Care District, Jyväskylä Medical Centre, Jyväskylä, Finland*

[6]*Docrates Hospital, Helsinki, Finland*

[7]*Department of Oncology and Metabolism, University of Sheffield, Sheffield, UK*

[#]*Contributed equally*

ARTICLE INFO

ABSTRACT

Krukenberg tumor (KT) is a rare subtype of ovarian neoplasms that manifests as secondary ovarian cancer. Most frequently, KTs originate from a primary in the gastrointestinal tract and account for 30 to 40% of all secondary ovarian cancers. A key histologic characteristic finding used in the diagnosis of KT is the presence of mucin-laden signet-ring cells. Bilateral metastasis into both ovaries has been reported in more than 80% of KTs, and a significant fraction of these cases are reported to receive no survival benefit from chemotherapy. Despite clinical evaluation of several chemotherapeutic treatments for the management of KT, the general prognosis of the disease is poor and radical surgery remains the main treatment shown to improve the overall survival. As no targeted therapies have been reported for KT, we performed an *ex vivo* drug screen to assess the efficacy of targeted therapeutics with patient-derived Krukenberg tumor cells. Tumor cells isolated from a coarse needle biopsy and tumor-associated immune cells derived from malignant ascites effusion from two patients with a gastric cancer derived KT were used for the analysis of responses to 120 drugs. A comparison of the results showed that tumor cells from both patients showed systematic sensitivity toward topoisomerase inhibition, epigenetic modulators, statins and alkaloid tubulin inhibitors. Ascites-derived immune cells displayed selective sensitivity to a number of targeted agents, including VEGFR inhibitor sunitinib. Flow cytometry analysis identified the effect of sunitinib to be immunomodulatory and targeted on the immunosuppressive M2 type macrophages. The immunomodulatory effect of sunitinib was confirmed from analysis of the patient ascites following treatment and was accompanied by sustained clinical response. These results support the concept of harnessing the immunomodulatory effects of VEGFR-TKI for cancer therapy and suggest further analysis also in the context of Krukenberg tumors.

Introduction

Krukenberg tumor (KTs) is a secondary ovarian cancer characterized by the presence of mucin-laden neoplastic signet-ring cells and stromal involvement [1]. Since there are also primary ovarian cancer subtypes that contain signet-ring cells with mucinous or nonmucinous material, for diagnosis, KT is distinguished from primary ovarian tumors that contain signet-ring cells with mucinous or nonmucinous material [2]. 10-

25% of all ovarian neoplasms are secondary cancers, and KT accounts for 3-10% of all ovarian neoplasms [3, 4]. The most common origin of KT is gastric cancer (up to 70% of cases), and gastric origin is associated with a poorer prognosis compared to KT with other primary tumors [5-7]. Ovarian metastasis of gastric cancer is also among the most important causes of treatment failure for gastric cancer in female patients [8]. Several treatments have been evaluated for the treatment of KT, and although systemic chemotherapy has been reported to provide prolonged survival in a subset of KT cases, the efficiency and prognosis remain poor, with most patients dying within a year of diagnosis [1, 2, 9, 10]. Radical cytoreductive surgery has been reported in several studies as the only treatment improving the overall survival for patients with gastric cancer derived KT [2, 11, 12]. However, there is discrepancy in the results for the benefits of radical cytoreductive surgery for gastric cancer derived KT, and it is likely beneficial only for a subset of patients [13, 14]. As no curative treatments and no targeted therapies have been described for KT, alternative treatments would be urgently needed to improve the treatments and survival outcome of patients affected with Krukenberg tumors.

In this study, we report the first described *ex vivo* analysis of drug sensitivity in Krukenberg tumors. Patient-derived tumor cells and immune cells isolated from malignant ascites from two patients with a gastric cancer derived KT were analysed to assess general drug sensitivities of KT cells beyond the currently used chemotherapies (Figure 1). *Ex vivo* drug screening allows assessment of the therapeutic efficacy of hundreds of drugs in parallel directly with patient-derived cell cultures [15-17]. This makes high-throughput *ex vivo* drug screening an attractive approach for biomarker discovery and assessment of patient-specific therapy sensitivity, especially in rare cancers for which clinical evaluation of novel therapies is difficult due to the low number of cases. Evidence from *ex vivo* screening can be used for the development of n-of-1 style trials, which may be the only option for clinical demonstration of targeted therapies in rare cancers [17, 18].
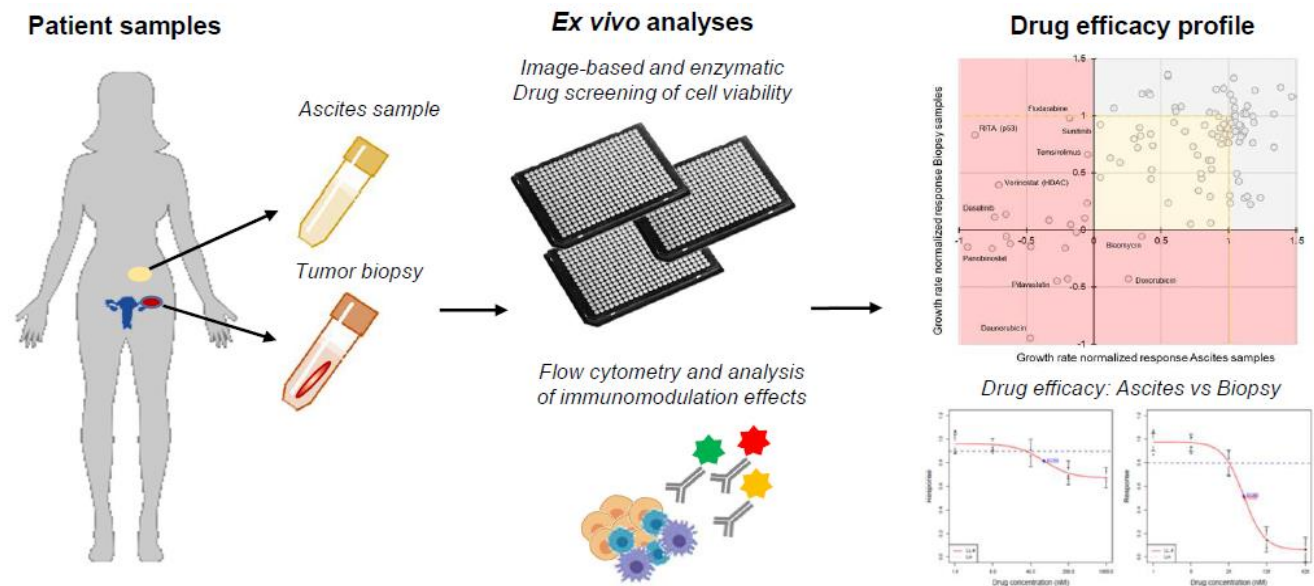

Figure 1: Illustration of the *ex vivo* assay strategy for Krukenberg tumors. Primary cell cultures are prepared from fresh patient tumor and malignant ascites samples as personalized *ex vivo* models. High-throughput single agent drug screens are performed with image-based assay for tumor tissue derived cells and an enzymatic viability assay is used for ascites derived cells. Immunophenotyping with flow cytometry is performed for sample cell characterization. Results are compared to nominate therapeutic strategies.

Findings from our study elucidate how KT tissue derived tumor cells respond to different chemotherapeutics and targeted pathway antagonism and how these same drugs affect the immune cells present in the malignant ascites fluid accumulating in the patient's peritoneal cavity. The results help in understanding how different cancer therapeutics affect the tumor and immune cells in parallel and how we may use this information to predict the patients´ responses to therapy, including immunomodulation effects to tailor personalized treatments for Krukenberg tumors and beyond.

Materials and Methods Patients

Patient 1 (Pt1), a 37-year-old female diagnosed with a stage IV gastric cancer with bilateral Krukenberg tumor metastasized to both ovaries. Metastases were inoperable, and the patient was referred for systemic therapy. Treatment prior to the *ex vivo* test had consisted of 8 rounds of FLOT regimen (fluorouracil, leucovorin, oxaliplatin, and docetaxel). Whole-body CT imaging after the treatments showed disease progression accompanied by rapid accumulation of malignant ascites fluid. The patient was then considered for further molecular pathology profiling and the *ex vivo* therapy sensitivity study. Patient 2 (Pt2), a 49-year old female diagnosed with a HER2+ gastric adenocarcinoma with bilateral Krukenberg tumor metastasized to both ovaries. Prior to the *ex vivo* test, the patient was treated with a combination regimen consisting of HER2 targeted drug, taxane and platinum compounds. Patient had an allergic reaction to paclitaxel. She received four cycles of nab-paclitaxel, carboplatin and trastuzumab before response evaluation. Clinically, she did not benefit from the treatment and whole-body CT scan after four cycles indicated disease progression. The patient was then considered for further molecular pathology profiling and the *ex vivo* therapy sensitivity study. Needle biopsy samples and 2 liters of malignant ascites

fluid were collected for the *ex vivo* drug screening with approval from the local Ethics Committee of the Central Finland Health Care District (KSSHP 3U/2015). All the experiments were undertaken with the understanding and written consent of the patients, and the study methodologies conformed to the standards set by the Declaration of Helsinki.

I Tumor Tissue Derived Primary Cell Cultures

One (Pt1) and two (Pt2) 18-gauge coarse needle biopsy cores sampled from the metastatic lesion in the ovary were devoted to establishing a vital primary tumor cell culture. The tissue cores were placed in sterile RPMI-1640 medium (Gibco) without supplements for transport to the research laboratory. Immediately upon receipt, the live tissue samples were washed three times with sterile PBS and finely cut to 2-5mm^3 pieces in sterile cell culture medium using scalpels. The primary bulk cell suspension dissociated from the tumor tissue during cutting was collected into a sterile centrifuge tube. The remaining tissue fractions were then placed into 1 mL of Accutase cell dissociation reagent (Gibco) per tissue and incubated at room temperature for 60 minutes. Following the enzymatic dissociation, the resulting cell suspensions and the initial cell suspension from the tissue cutting plates were combined, collected with centrifugation and subjected to filtration through a 70µm cell strainer (pluriSelect Life Science UG) in sterile RPMI-1640 medium. The resulting cell suspension was quantified using a Cellometer Mini cell counter (Nexcelom). The suspension was diluted to RPMI-1640 medium containing 5% FBS to achieve a suspension with 1,000 cells per 45µL medium. The cells were then immediately dispensed into drug-containing 384-well plates and incubated in normal cell culture conditions for 120 hours (37°C, 5% CO2).

II Ascites Fluid Derived Primary Cell Cultures

Malignant ascites fluid was drained as a palliative procedure, and 200ml of the fluid was collected with the aim to isolate the fluid contained cells for *ex vivo* drug screening. The fluid was centrifuged at room temperature in four 50ml conical bottom centrifuge tubes for 5 minutes at $200 \times g$. The cell pellets were re-suspended in 1ml of sterile PBS (Gibco) and diluted 1:10 in 1× ACK Lysing Buffer (Gibco) for 5 minutes to lyse the red blood cells. Samples were then centrifuged at room temperature in 15ml conical bottom centrifuge tubes for 5 minutes at 200 × g, and the resulting cell pellet was re-suspended into 5ml of sterile RMPI-1640 medium (Gibco) supplemented with 5% FBS and quantified with an automated cell counter as above. Cell counting indicated an initial cell density of 1×10^4 per ml of ascites fluid from Pt1 sample and an excess of 1×10^6 cells per ml of ascites fluid for Pt2. Cell suspensions were subjected to filtration through a 70µm cell strainer and diluted to 5% FBS containing RPMI-1640 medium to achieve a final suspension with 5,000 cells per 45µL medium. The cells were then immediately dispensed into drug-containing 384-well plates and incubated in normal cell culture conditions for 120 hours (37°C, 5% CO2). The excess cells were pelleted and frozen in cell freezing medium (MP Biomedicals).

III Image-Based High Content Drug Screening

The image-based drug screening was performed as previously described [16, 17]. Briefly, the therapeutic compound collection consisted of 120

anti-cancer agents (Supplementary Table 1) tested with four 2-fold dilutions starting from 5 micromolar as the highest concentration. The single-cell suspensions (45 µl per well; 1,000 cells per well) were transferred to each 384-well using an automated Multidrop-384 peristaltic dispenser (ThermoScientific). The 384-well plates were incubated for 120 h at standard cell culture conditions. Analysis of cell viability from the biopsy samples was performed through high-content imaging. The cell cultures were fixed and stained as detailed before. Antibody against epithelial cell marker cytokeratin-19 (KRT19, Abcam, Clone EP1580Y) was used for the staining of cells of epithelial origin. DAPI (4',6- Diamidino-2-phenylindole nuclear counterstain, LifeTech) was used for DNA counterstaining to allow image cytometry and cell counting. Cells were imaged on the Olympus scan^R platform at 10X magnification. 6 frames were acquired from each 384-well. Images were analysed with Olympus scan^R image analysis suite, including DNA staining-based primary object segmentation using a watershed algorithm. Cell count data was normalized to DMSO-only wells (negative control) and 2µM aphidicolin- containing wells (cell growth control) to allow for growth rate normalized dose-response scoring [17].

IV Enzymatic Cell Viability Assays

The e*x vivo* drug screens and the cell viability assays with the malignant ascites derived cells was performed by an enzymatic cell viability assay determining the total ATP (adenosine triphosphate) levels as a surrogate for quantification of the live cells per well (CellTiter-Glo luminescent cell viability assay, Promega). 15µl of the reagent was added per well and incubated for 15 at room temperature with gentle shaking. Luminescence was then measured using a Labrox luminescence plate reader (Labrox, Turku, Finland). Growth rate normalized dose responses were calculated as detailed above.

V Flow Cytometry Analysis

Flow cytometry was used for immune cell profiling and evaluation of cell type specific phenotypes from the ascites samples. Ascites derived cells from Pt2 were analysed before and after treatment with sunitinib and following 48-hour *ex vivo* treatment with 2.5µM sunitinib. The analysis was performed using the following monoclonal antibodies (mAb): anti-CD45-PerCP-Cy5.5, anti-CD14-Pacific Blue, anti-CD16-PE, anti- CD56-PE, anti-CD4-PE-Cy7, anti-CD8-APC-Cy7, anti-CD19-APC, anti–HLAII-DR-FITC, anti-CD163-PerCP-Cy7 and anti-Clever-1 (Stab1)-Pacific Blue. Monoclonal antibodies anti-IgG1-APC and anti-IgG1-PE (BioLegend) were used as isotype controls. Anti-Clever-1 (Stab1) antibody was purchased from InVivo Biotech, and all other mAbs were purchased by BD Biosciences and BioLegend. Staining was done on live cells with a viability dye (eFluor 450 or eFluor 780; Invitrogen) and stained with conjugated primary antibodies without fixation. Flow cytometric analysis was performed using LSRFortessa (BD Biosciences) and analysed with FlowJo 10 (TreeStar).

VI Statistical Analysis

The *ex vivo* drug screening data were analysed using the normalized growth rate inhibition (GR) approach, which yields per-division metrics for drug potency (GR50) and efficacy (GRmax) [19]. Dose-response curves for growth rate normalized GR50, and IC50 estimates were

generated in GraphPad Prism software (V7, GraphPad Software Inc.).Welch's t-test and Pearson correlation analyses were applied using GraphPad Prism software, as indicated in the figure legends according to assumptions on data normality.

Results

I *Ex Vivo* Drug Efficacy Screening

Patients who participated in the study by donating the tumor and ascites samples were initially treated with several cycles of usually effective chemotherapy. Patient 1 had received 8 rounds of treatment with docetaxel, fluorouracil and oxaliplatin (FLOT) prior to the *ex vivo* test. Patient 2 had been treated with trastuzumab, nab-paclitaxel and carboplatin. In both cases, the disease progressed through the chemotherapies with no obvious clinical benefit. At this stage, tumor biopsies and a sample of malignant ascites fluids were received for the

purpose of *ex vivo* therapy efficacy screening. For the *ex vivo* drug screening experiment, the tissue and ascites samples were processed immediately on the day of biopsy and the ascites puncture. Using standard techniques to establish primary cell cultures from tumor tissues, a primary culture was prepared from the patients' tumor tissue, while the ascites contained cells were collected with simple centrifugation without enrichment of any selected cell type [17]. These bulk tumor cell samples were then plated directly onto drug-containing 384-well microplates in a milieu of different cell types and incubated with 120 drugs in four doses for 5 days before viability measurements. Viability assay for the tumor tissue derived adherent cells was done with an image-based cell counting assay [17]. Cells were fixed and stained with a gastric cancer associated epithelial cell lineage marker cytokeratin-19 (KRT19), and automated microscopy and image analysis were used to quantify cell growth and viability on the basis of imaging cytometry (Figures 1 & 2C) [20].
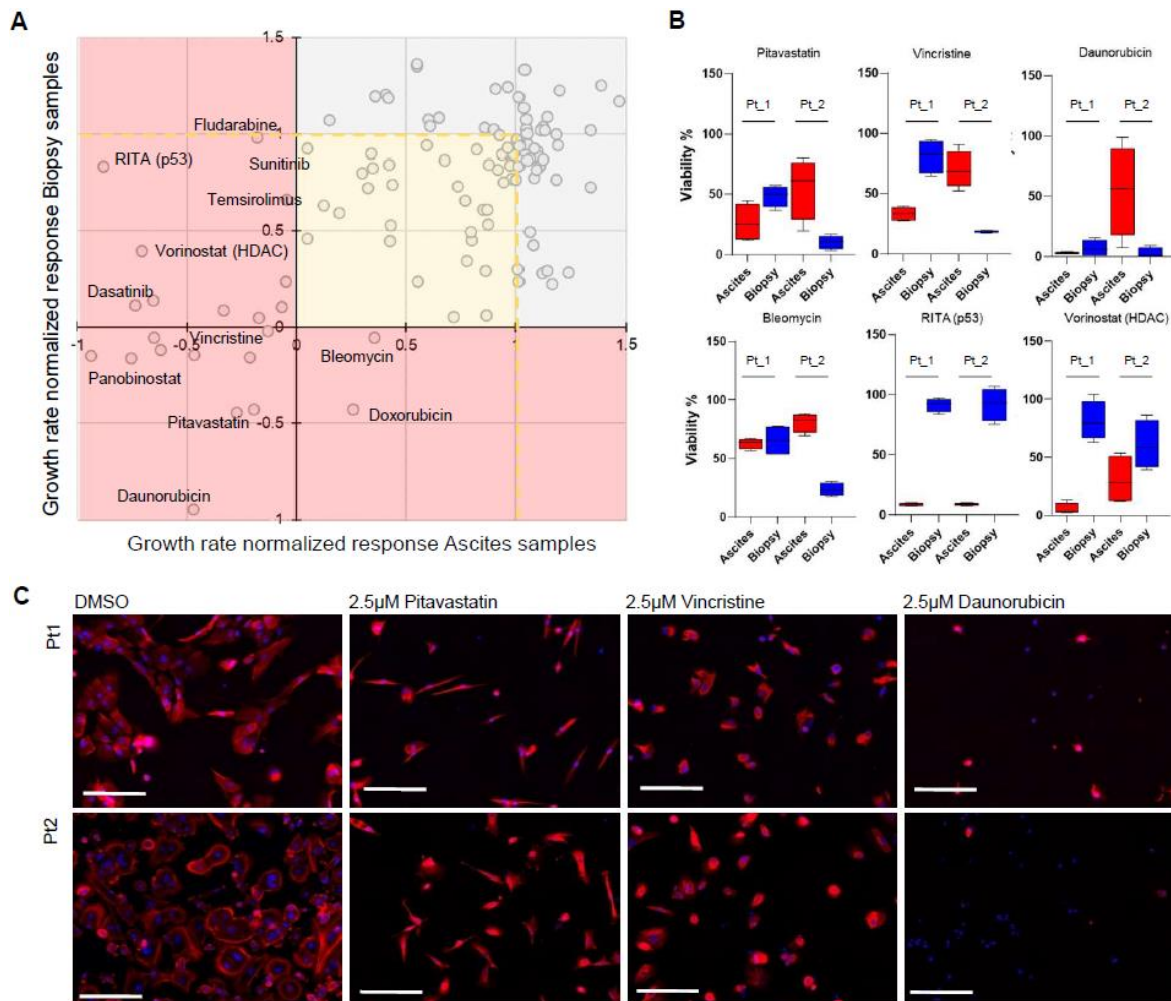

Figure 2: *Ex vivo* high-throughput drug screens with tumor and malignant ascites derived cell types. **A)** Scatter plot for comparison of the growth rate normalized drug efficacy on the tumor and malignant ascites derived cell cultures. Results from both patients were combined to identify common and differential drug responses between the tumor and ascites derived cells. **B)** The drug screens demonstrated that cells from tumor tissues were differentially responsive to selected chemotherapeutic drugs, including topoisomerase inhibitors. Ascites derived cells demonstrated selective sensitivity to several classes of targeted agents, including inhibitors of VEGFR, mTOR, p53 (RITA) and HDAC (vorinostat). Box plots showing the % viability for the 4 drug doses tested with each sample. **C)** Fluorescence microscopy images from the image- based drug screens showing Pt1 and Pt2 tumor tissue derived cells following 120 h exposure to DMSO and 2.5µM pitavastatin, vincristine and daunorubicin. KRT19 staining shown in red, DNA in blue. Scale bars 100µm.

Both Pt1 and Pt2 tumor tissue derived cells displayed strong uniform staining of KRT19 in >90% of the cells. The morphology of the Pt1 and Pt2 cells differed, though clearly with a large fraction of the Pt2 tumor derived cells having a distinct large round shape (Figure 2C) fitting well with that of the signet-ring cells characteristic to KT [5]. In comparison of the negative control cells (DMSO treatment) and aphidicolin treated cells, the estimated cell-doubling rate of Pt1 tumor tissue derived cells was calculated to be ~210 hours corresponding to 0.6 cell division over the course of the 120-hour screening assay [19]. The estimated cell-doubling rate of Pt2 tumor tissue derived cells was calculated to be ~70 hours corresponding to 1.7 cell division over the course of the assay. With the cells isolated from the malignant ascites fluids, the cell viability assay was performed with an enzymatic assay as large fraction of the cells had not adhered to the microwells during the 120-hour assay. On the basis of the control samples, the estimated cell-doubling rate of Pt1 ascites derived cells was calculated to be ~152 hours and 146 hours for Pt2. The cell division rates of the samples were used for calculation of growth rate normalized GR dose responses to allow comparison of the drug sensitivity profiles between the patients and the different sample types (Figures 2A & 2B).

To identify the most potent common and selective growth inhibitory and cytotoxic drug responses between the two patients and the different sample cell types, we averaged the GR metrics of the drugs from the two patients separately for the tumor tissues and ascites derived cells (Supplementary Table 1) (Figure 2A). Using a stringent ranking criterion where the average of the GR values across the four drug doses and both patients had to be stronger than GR=0 (the cell growth stalling effect of aphidicolin), we identified 12 drugs having a strong cytotoxic effect on the tumor derived cells. Pitavastatin, a cholesterol-lowering drug, was among these most potent cytotoxic drugs together with 5 topoisomerase inhibitors (Figures 2A & 2C). 16 drugs had a cytotoxic effect (GR <0) on the ascites derived cells, including two mTOR inhibitors, dasatinib, and several nucleoside antimetabolite drugs used for treatment of hematological cancers (Figure 2A). The most strikingly different cytotoxic effect was seen with RITA (NSC652287), a small molecule re-activator of p53 that induces apoptosis primarily in the context of a p53 wild type genetic background (Figure 2B) [21].
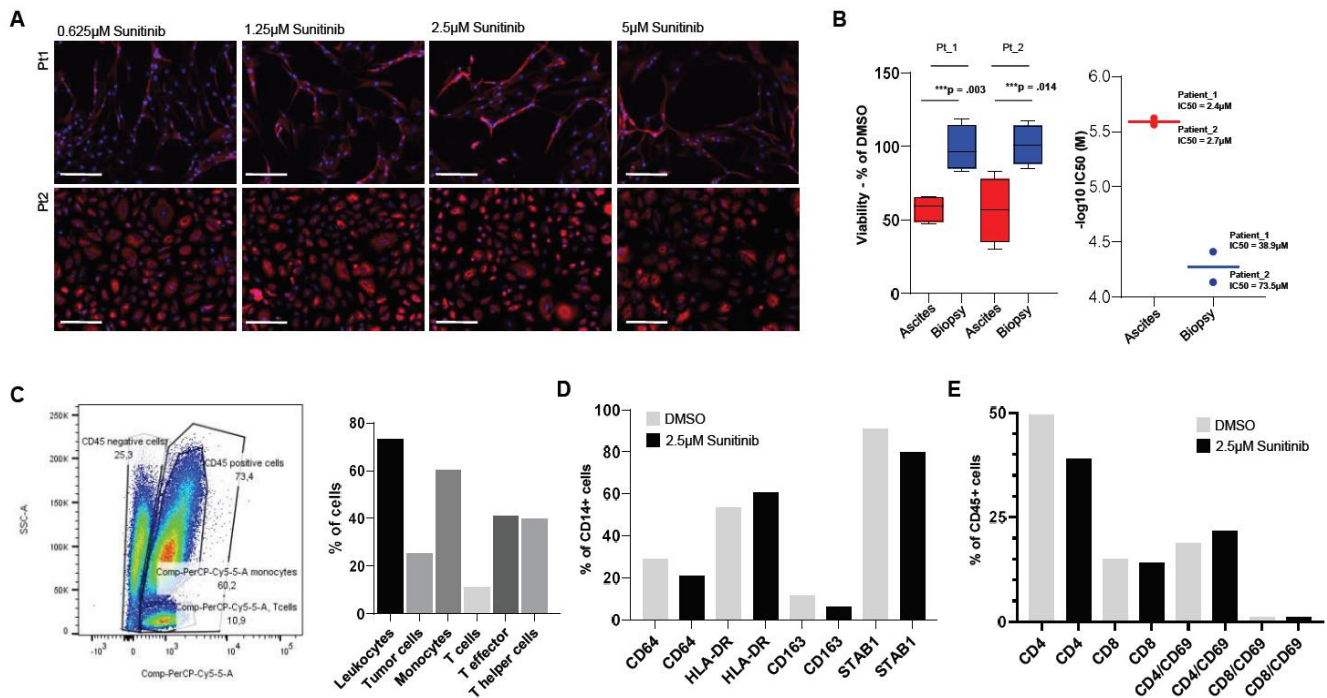

Figure 3: Differential response of the malignant ascites cells to sunitinib was derived from responses of the tumor associated macrophages (TAMs). **A)** Gallery of the phenotypes of tumor tissue derived cells to sunitinib from Pt1 and P2. Scale bars 100µm. **B)** Left, box plot showing % viability values of the ascites and tumor derived cells to sunitinib. Right, comparison of the sample type specific IC50 estimates for sunitinib on Pt1 and Pt2 samples (-log10 IC50 (M). **C)** Flow cytometry profiling of the cellular composition of Pt2 malignant ascites. **D)** Sunitinib modulates macrophage phenotypes *ex vivo*. The % values of phenotypic marker defined immune cell populations following exposure of the ascites cells to DMSO and 2.5µM sunitinib. **E)** Flow cytometry profiling of T-cell phenotype markers in response to 2.5µM sunitinib.

II Analysis of The Malignant Ascites Derived Cells

10 out of the 120 drugs were selectively cytotoxic for the cells derived from the malignant effusions (Supplementary Table 1). In addition, a number of pathway-targeted drugs had a more potent growth inhibitory effect on the ascites cells. These included JAK inhibitor ruxolitinib, STAT inhibitor fludarabine, Bcr-Abl inhibitors bosutinib, nilotinib, and

5 VEGFR/PDGFR inhibitors, including sunitinib, which had no cytotoxic effect on the tumor tissue derived cells (Figures 3A & 3B). All these drugs and the antagonism of their corresponding target pathways are associated with targeting various immune cell types. Malignant ascites is one of the major clinical features of KT and the main cellular components of malignant ascites is the immune cells [2, 22]. To dissect the selective growth inhibitory effect of these drugs with respect to the

cellular composition of the ascites samples used in the drug screening, excess cells that were frozen from the initial Pt2 ascites sample were subjected to flow cytometry profiling. The analysis revealed that 75% of the ascites derived cells were CD45 positive leukocytes, 60% were monocytes, 11% were T-cells, and 25% were CD45 negative tumor/stromal cells (Figure 3C & Supplementary Figure 1). Of the CD45 positive monocytes, ~79% were CD14 positive (Figures 3C & 4A), and from the T-cells, ~41% were CD8 positive T-effector cells and ~39% were CD4 positive T-helper cells (Figure 3C & Supplementary Figure 1).

As the most abundant cellular component in the ascites were the immunosuppressive CLEVER1/STAB1 positive CD14 positive M2 type macrophages (75% of CD14$^+$ monocytes), we sought to test what effects the ascites selective growth inhibitory drugs have on this tumor-associated macrophage (TAM) population [23]. Sunitinib was initially identified to have a potent growth inhibitory impact on the ascites samples of both patients (Figure 3B) and no cytotoxic effect on the tumor-derived cells (Figure 3A). To validate the effect of sunitinib, ascites cells from the Pt2 sample were seeded on low adhesion cell culture 6-well plates and treated with DMSO or 2.5µM sunitinib for 48 hours in standard cell culture conditions. The cells were analysed using separate antibody panels for M1/M2 macrophage polarization and T-cell activation [23, 24]. Treatment of the ascites cells with sunitinib resulted in ~20% reduction of the total number of viable cells accompanied with ~30% reduction of CD64 positive macrophages, ~13% increase in the number of HLA-DR positive activated M1 type macrophages, ~10% decrease of CD163 positive M2 type macrophages and ~13% decrease of STAB1 positive M2 type macrophages (Figure 3D & Supplementary

Figure 2). The amount of CD4 positive T-cells was reduced by ~22% and CD8 positive T-cells by ~7%. The amount of CD4/CD69 positive T-cells was increased by ~12%, indicating modest activation of T-cells in response to the exposure of the cells to sunitinib (Figure 3E & Supplementary Figure 2).

III *Ex Vivo* Informed Treatment

For KT, there are no standard second-line treatment guidelines, and no suitable clinical trials existed for these patients at the time of this study. For patient 1, the general health condition did not suffice for further treatment attempts, and she succumbed to the disease shortly after stopping of active treatment. For patient 2, the general health condition still allowed for a treatment to be attempted at the time of this study, and she was considered for an experimental therapeutic approach informed by the *ex vivo* screening. After clinical evaluation and based on the detected immunomodulatory effect of sunitinib that resulted in the reduction of the amount of immunosuppressive STAB1$^+$ M2 type macrophages *ex vivo* (Figure 3D), the patient was initiated off-label treatment with sunitinib. Dosing and treatment schedules for sunitinib were adapted from renal cell cancer indication. Following four weeks of treatment, the ascites fluid accumulation had stopped, and the patient reported improvement of the quality of life and reduction of pain. During a follow-up visit to the clinic, a puncture was performed to collect a small sample of the residual ascites fluid to analyze the cellular contents of the fluid. A flow cytometry analysis was performed on the sample to compare the general cellular composition in the fluid and the amount of immunosuppressive STAB1 expressing macrophages, which were the predominant cell type in the pre-treatment sample (Figure 4A).
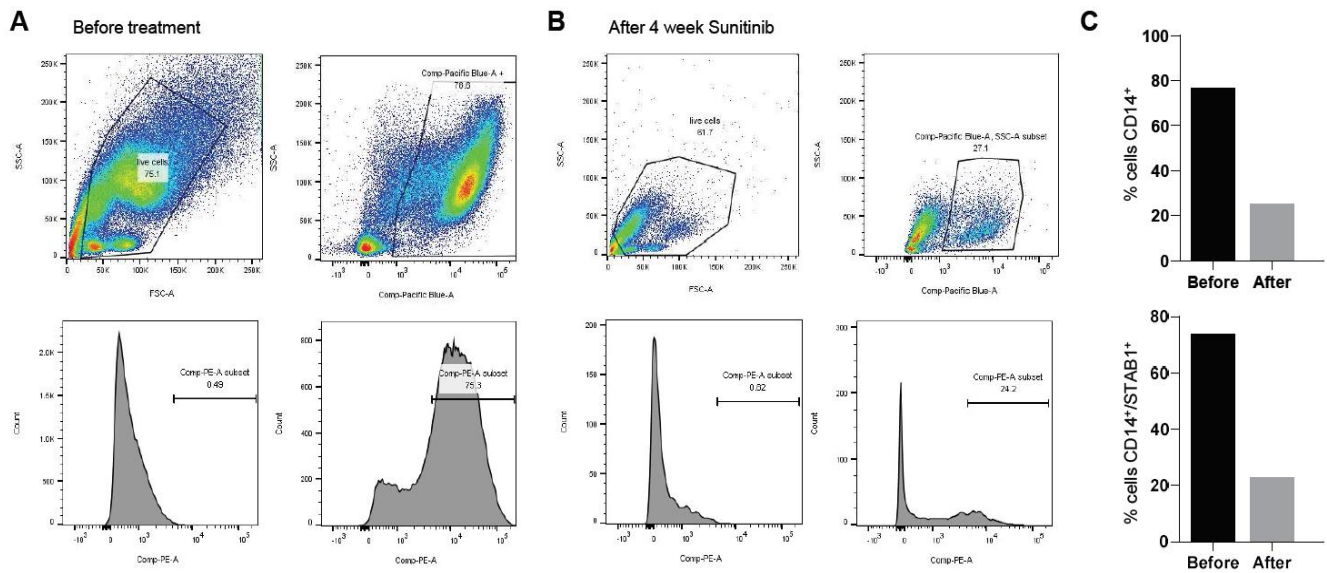

Figure 4: Sunitinib treatment modulated the immunosuppressive cell composition of malignant ascites by reducing the amount of immunosuppressive STAB1 positive immunosuppressive macrophages. **A)** Flow cytometry analysis of STAB1 expressing CD14 positive monocytes from patient ascites before treatment. **B)** Analysis of STAB1 expressing CD14 positive monocytes following four weeks treatment with sunitinib. **C)** Frequencies of CD14+ monocytes and CD14+/STAB1+ immunosuppressive TAMs as percentage of malignant ascites derived cells before and after sunitinib treatment.

Before sunitinib treatment, 75.3% of the ascites derived CD14 positive monocytes expressed STAB1 (MFI 23416, Figure 4C). After 4 weeks of treatment with sunitinib (Figure 4B), 27.1% of the ascites derived cells were CD14 positive (78.6% before treatment), and 24.2% of these

expressed STAB1 (MFI 12356, Figure 4C). These results indicated that during the treatment, the total amount of CD14 positive monocytes had been reduced by nearly 50% and that the treatment had resulted in 68% reduction of the amount STAB1 expressing immunosuppressive CD14+

monocytes (Figure 4C). Treatment of patient 2 was then continued with sunitinib, fluvastatin and trastuzumab. She continued to receive clinical benefit from the treatment for six months. Radiological response evaluation with a CT scan was performed 2 and 5 months after initiating *ex vivo*-informed treatment. Both these scans indicated stable disease according to RECIST 1.1 criteria. 6 months after initiating treatment, ascites started accumulating again, and new subcutaneous metastatic lesions were observed. At that point, fluvastatin and sunitinib were stopped. Trastuzumab was continued for 2 more cycles despite clinical progression. The patient did not get clinical benefit from trastuzumab, was switched to the best palliative care and succumbed to the disease 12 months after initiation of the *ex vivo*-informed treatment.

Discussion and Conclusion

The prognosis for KTs of gastrointestinal tract origin is poor, and most patients die within 1 year after diagnosis of ovarian metastasis [2]. KTs are associated with extensive malignant spread within the abdominal cavity, and surgical intervention is possible only for a subset of patients. Indeed, radical cytoreductive surgery is the only treatment shown to improve the overall survival of KT patients. Chemotherapeutic drugs that offer improved tumor response rates in gastrointestinal tract neoplasms generally have low antineoplastic activity for metastases in the ovaries [10]. Alternative treatment strategies are, therefore, urgently needed to improve the management and overall survival of patients affected with Krukenberg tumors.

We report here the first described *ex vivo* study and clinical use of drug efficacy testing in Krukenberg tumors. With the aim to model therapeutic efficacy for advanced gastric primary derived KT, we performed a comparative analysis of drug effects on tumor tissue derived primary tumor cell cultures and malignant ascites derived immune cells from two KT patients. The drug screens were initiated on the day of tissue sampling, and the screening results were available just five days after sampling of the tissues. This shows that *ex vivo* drug screening can be used as a rapid technique to complement pathological and clinical diagnostics and to identify alternative treatment strategies where standard therapeutic options have been exhausted. The comparative analysis of the tumor and the ascites derived cells yielded dose and target dependent drug response profiles that could be linked to specific cell types; the tumor tissue derived epithelial cells and the malignant ascites derived cell types. In more detail, we identified drugs potentially having immunomodulatory effects on the immunosuppressive M2 type TAMs present in high numbers in the malignant ascites. The role of the immunosuppressive macrophages in the malignant ascites of KT patients has not been studied, but in the context of epithelial ovarian cancers, the amount and ratio of M2 type immunosuppressive TAMs over the inflammatory M1 type macrophages have been shown to associate with worse prognosis [24-26].

The identified immunomodulatory effect of sunitinib on the STAB1 positive immunosuppressive macrophages supports other studies where the therapeutic effects of VEGFR-TKIs such as sunitinib, sorafenib and pazopanib, as well as mTOR inhibitors, has been suggested to occur via their impact on the immune cells [27-29]. The effects of these pathway-antagonizing drugs have the potential to switch the balance between immunosuppression and immune activation in the tumor

microenvironment and result in activation of antitumor immune responses and improve response also to other treatment, particularly for immune-based treatments [30-32]. Therapeutic strategies to targeted TAMs as core regulators of cancer-related inflammation and immunotherapeutic resistance have thus started to attract major interest as novel immunotherapeutic strategies for cancer treatment. Clinical development of several strategies to target immunosuppressive macrophage is underway [33].

In summary, by interrogating patient-derived cells in this *ex vivo* study, we identify a number of anti-cancer drugs that could be beneficial for the treatment of KTs. Tumor cells isolated from the patients' tumor tissue were attempted to be cultured *in vitro* following the drug screening, but cells from both patients eventually stopped dividing following the initial 2-3 passages. Primary patient-derived tissue cultures thus still remain the only option for performing experimental *in vitro* research with KT derived tumor cells. No established cell lines have been described from Krukenberg tumors. The results obtained from analyses performed with the malignant ascites derived immune cells also suggest that the ascites derived cells could be used as models for assessment of patient-specific immunotherapeutic drug effects, which could prove to be highly useful in the emerging era of immune-oncology therapies.

Acknowledgements

REFERENCES

1. Matsushita H, Watanabe K, Wakatsuki A (2016) Metastatic gastric cancer to the female genital tract. *Mol Clin Oncol* 5: 495-499. [Crossref]
2. Kubeček O, Laco J, Špaček J, Petera J, Kopecký J et al. (2017) The pathogenesis, diagnosis, and management of metastatic tumors to the ovary: a comprehensive review. *Clin Exp Metastasis* 34: 295-307. [Crossref]
3. Fujiwara K, Ohishi Y, Koike H, Sawada S, Moriya T et al. (1995) Clinical implications of metastases to the ovary. *Gynecol Oncol* 59: 124-128. [Crossref]
4. Moore RG, Chung M, Granai CO, Gajewski W, Steinhoff MM (2004) Incidence of metastasis to the ovaries from nongenital tract primary tumors. *Gynecol Oncol* 93: 87-91. [Crossref]
5. AlAgha OM, Nicastri AD (2006) An in-depth look at Krukenberg tumor: an overview. *Arch Pathol Lab Med* 130: 1725-1730. [Crossref]
6. Jiang R, Tang J, Cheng X, Zang RY (2009) Surgical treatment for patients with different origins of Krukenberg tumors: outcomes and prognostic factors. *Eur J Surg Oncol* 35: 92-97. [Crossref]
7. Yu P, Huang L, Cheng G, Yang L, Dai G et al. (2017) Treatment strategy and prognostic factors for Krukenberg tumors of gastric origin: report of a 10-year single-center experience from China. *Oncotarget* 8: 82558-82570. [Crossref]

8. Rosa F, Marrelli D, Morgagni P, Cipollari C, Vittimberga G et al. (2016) Krukenberg tumors of gastric origin: the rationale of surgical resection and perioperative treatments in a multicenter western experience. *World J Surg* 40: 921-928. [Crossref]

9. Kim HK, Heo DS, Bang YJ, Kim NK (2001) Prognostic factors of Krukenberg's tumor. *Gynecol Oncol* 82: 105-109. [Crossref]

10. Brieau B, Auzolle C, Pozet A, Tougeron D, Bouché O et al. (2016) Efficacy of modern chemotherapy and prognostic factors in patients with ovarian metastases from gastric cancer: a retrospective AGEO multicentre study. *Dig Liver Dis* 48: 441-445. [Crossref]

11. Lu LC, Shao YY, Hsu CH, Hsu C, Cheng WF et al. (2012) Metastasectomy of Krukenberg tumors may be associated with survival benefits in patients with metastatic gastric cancer. *Anticancer Res* 32: 3397-3401. [Crossref]

12. Cho JH, Lim JY, Choi AR, Choi SM, Kim JW et al. (2015) Comparison of surgery plus chemotherapy and palliative chemotherapy alone for advanced gastric cancer with Krukenberg tumor. *Cancer Res Treat* 47: 697-705. [Crossref]

13. Lionetti R, De Luca M, Travaglino A, Raffone A, Insabato L et al. (2019) Treatments and overall survival in patients with Krukenberg tumor. *Arch Gynecol Obstet* 300: 15-23. [Crossref]

14. Ma F, Li Y, Li W, Kang W, Liu H et al. (2019) Metastasectomy Improves the Survival of Gastric Cancer Patients with Krukenberg Tumors: A Retrospective Analysis of 182 patients. *Cancer Manag Res* 11: 10573-10580. [Crossref]

15. Kettunen K, Boström PJ, Lamminen T, Heinosalo T, West G et al. (2019) Personalized Drug Sensitivity Screening for Bladder Cancer Using Conditionally Reprogrammed Patient-derived Cells. *Eur J Urol* 76: 430-434. [Crossref]

16. Lehtomaki KI, Lahtinen LI, Rintanen N, Kuopio T, Kholova I et al. (2019) Clonal Evolution of MEK/MAPK Pathway Activating Mutations in a Metastatic Colorectal Cancer Case. *Anticancer Res* 39: 5867-5877. [Crossref]

17. Arjonen A, Mäkelä R, Härmä V, Rintanen N, Kuopio T et al. (2020) Image-based ex vivo drug screen to assess targeted therapies in recurrent thymoma. *Lung Cancer* 145: 27-32. [Crossref]

18. Billingham L, Malottki K, Steven N (2016) Research methods to change clinical practice for patients with rare cancers. *Lancet Oncol* 17: e70-e80. [Crossref]

19. Hafner M, Niepel M, Chung M, Sorger PK (2016) Growth rate inhibition metrics correct for confounders in measuring sensitivity to cancer drugs. *Nat Methods* 13: 521-527. [Crossref]

20. Kim MA, Lee HS, Yang HK, Kim WH (2004) Cytokeratin expression profile in gastric carcinomas. *Hum Pathol* 35: 576-581. [Crossref]

21. Issaeva N, Bozko P, Enge M, Protopopova M, Verhoef LG et al. (2004) Small molecule RITA binds to p53, blocks p53-HDM-2 interaction and activates p53 function in tumors. *Nat Med* 12: 1321-1328. [Crossref]

22. Ahmed N, Stenvers KL (2013) Getting to know ovarian cancer ascites: opportunities for targeted therapy-based translational research. *Front Oncol* 3: 256. [Crossref]

23. Viitala M, Virtakoivu R, Tadayon S, Rannikko J, Jalkanen S et al. (2019) Immunotherapeutic Blockade of Macrophage Clever-1 Reactivates the CD8+ T-cell Response against Immunosuppressive Tumors. *Clin Cancer Res* 25: 3289-3303. [Crossref]

24. Zhang M, He Y, Sun X, Li Q, Wang W et al. (2014) A high M1/M2 ratio of tumor associated macrophages is associated with extended survival in ovarian cancer patients. *J Ovarian Res* 7: 19. [Crossref]

25. Reinartz S, Schumann T, Finkernagel F, Wortmann A, Jansen JM et al. (2014) Mixed-polarization phenotype of ascites- associated macrophages in human ovarian carcinoma: correlation of CD163 expression, cytokine levels and early relapse. *Int J Cancer* 134: 32-42. [Crossref]

26. Yafei Z, Jun G, Guolan G (2016) Correlation between macrophage infiltration and prognosis of ovarian cancer- a preliminary study. *Biomed Res* 27: 305.

27. Kumar R, Crouthamel MC, Rominger DH, Gontarek RR, Tummino PJ et al. (2009) Myelosuppression and kinase selectivity of multikinase angiogenesis inhibitors. *Br J Cancer* 101: 1717–1723. [Crossref]

28. Santoni M, Berardi R, Amantini C, Burattini L, Santini D et al. (2014) Role of natural and adaptive immunity in renal cell carcinoma response to VEGFR-TKIs and mTOR inhibitor. *Int J Cancer* 134: 2772-2777. [Crossref]

29. Zizzari IG, Napoletano C, Botticelli A, Caponnetto S, Calabrò F et al. (2018) TK Inhibitor Pazopanib Primes DCs by Downregulation of the β-Catenin Pathway. *Cancer Immunol Res* 6: 711-722. [Crossref]

30. Draghiciu O, Nijman HW, Hoogeboom BN, Meijerhof T, Daemen T (2015) Sunitinib depletes myeloid-derived suppressor cells and synergizes with a cancer vaccine to enhance antigen-specific immune responses and tumor eradication. *Oncoimmunology* 4: e989764. [Crossref]

31. Tamura R, Tanaka T, Akasaki Y, Murayama Y, Yoshida K et al. (2019) The role of vascular endothelial growth factor in the hypoxic and immunosuppressive tumor microenvironment: perspectives for therapeutic implications. *Med Oncol* 37: 2. [Crossref]

32. Zemek RM, Chin WL, Nowak AK, Millward MJ, Lake RA et al. (2020) Sensitizing the Tumor Microenvironment to Immune Checkpoint Therapy. *Front Immunol* 11: 223. [Crossref]

33. Cassetta L, Pollard J (2018) Targeting macrophages: therapeutic approaches in cancer. *Nat Rev Drug Discov* 17: 887-904. [Crossref]